



Faraday rotation of pure and transition metal-doped zinc selenide

R. Shahin¹ · O. V. Martynova¹ · S. V. Kurashkin^{1,2} · A. P. Savikin¹

Received: 24 November 2023 / Accepted: 17 March 2024 / Published online: 5 April 2024
© The Author(s), under exclusive licence to Springer-Verlag GmbH Germany, part of Springer Nature 2024

Abstract

The current study is dedicated to measuring the Verdet constant of pure and chromium and iron ions doped ZnSe using laser sources in the range from 632.8 to 2430 nm. An increase in the magneto-optical properties of ZnSe as a result of diffusion doping with transition metal ions was experimentally discovered. The results align with the Van Vleck-Hebb theory, which predicts a nearly linear rise in the Verdet constant with increasing of transition element concentration.

1 Introduction

It is rare that a modern laser system does not incorporate a magneto-optical Faraday element, such as magneto-optical modulator, polarization switch, rotator or isolator [1]. The operation of these devices is based on the phenomenon of magnetically induced rotation of the polarization direction. There are quite a lot of magneto-optical materials applicable to the visible and near-IR regions, the properties of which have been well studied. One of the most important is terbium gallium garnet (TGG) used in both crystalline and ceramic forms. The TGG crystal possesses a large Verdet constant ($\sim 36 \text{ rad}/(\text{T}\cdot\text{m})$ at 1064 nm), high thermal conductivity ($7.4 \text{ W}/(\text{m}\cdot\text{K})$), low optical losses ($< 0.1\%/ \text{cm}$) and high laser damage threshold ($> 5 \text{ J}/\text{cm}^2 @ 10 \text{ ns}/1064 \text{ nm}$) [2, 3].

Currently, there is a limited number of magneto-active materials suitable for constructing Faraday devices for mid-IR lasers. In near-IR range, popular magneto-active materials are lanthanide fluorides and oxides (CeF_3 , PrF_3 , TbF_3 , Dy_2O_3 , Ho_2O_3 , etc.) in the form of single crystals or ceramics [4–8]. An established magneto-active material for low-power mid-IR lasers is the yttrium iron garnet (YIG) crystal and its rare-earth-substituted compositions [9]. These materials have high specific Faraday rotation and low saturation magnetization [1, 10]. However, their production uses

time-consuming processes such as the floating zone method or liquid phase epitaxy, that makes it difficult to obtain large-sized crystals and leads to high final costs of the Faraday device. Also, borate glasses doped with dysprosium [11] and tellurium-arsenic-selenium glasses [12] show a great promise for Faraday mid-IR devices. In these works, the room temperature Verdet constant at a wavelength of $1.94 \mu\text{m}$ was in the range of about $8\text{--}15 \text{ rad}/(\text{T}\cdot\text{m})$. The possibility of using single-crystal silicon as an effective Faraday insulator for a wavelength of $1.94 \mu\text{m}$ was shown in [13]; the measured Verdet constant for a wavelength of $1.94 \mu\text{m}$ was $15.2 \text{ rad}/(\text{T}\cdot\text{m})$. The advantages of this material include the possibility of producing large-diameter samples with relatively low absorption losses.

A good alternative to these materials can become polycrystalline materials based on zinc chalcogenides, which are relatively easy to manufacture and can be scaled up to several centimeters in aperture size [14]. Zinc chalcogenide crystals have a wide range of transparency ($0.4\text{--}12 \mu\text{m}$ for ZnS and $0.5\text{--}20 \mu\text{m}$ for ZnSe) and good magneto-optical properties. Thus, pure ZnSe polycrystals have a Verdet constant $V = 98.5 \text{ rad}/(\text{T}\cdot\text{m})$ at a wavelength of 632.8 nm, $28.3 \text{ rad}/(\text{T}\cdot\text{m})$ at a wavelength of 1064 nm and $7.7 \text{ rad}/(\text{T}\cdot\text{m})$ at a wavelength of 1940 nm [15]. In work [15], ZnSe was successfully used as a magneto-active material. Here, isolation of radiation with a wavelength of $1.94 \mu\text{m}$ and optical power of 20 W was obtained. In addition, to isolate radiation up to 200 W with the isolation ratio of the device of $\sim 25 \text{ dB}$ was demonstrated.

It is known that diffusion doping of zinc chalcogenide crystals with ions of transition elements from metal or spray pyrolysis deposited films makes it possible to obtain crystals of laser quality and the required concentration [16, 17]. That

✉ R. Shahin
ragheed.shaheen1@hotmail.com

¹ N.I. Lobachevsky Nizhny Novgorod State University, 23 Gagarin Avenue, 603022 Nizhny Novgorod, Russia

² G.G. Devyatykh Institute of Chemistry of High-Purity Substances of RAS, 49 Tropinina St., 603951 Nizhny Novgorod, Russia

leads to the idea, that in addition to their direct purpose as active elements of IR lasers, metal-doped chalcogenides can be of interest as magneto-active materials since the Faraday effect might be enhanced due to the presence of dopants. This assumption motivated us to conduct studies of the magneto-optical characteristics of ZnSe polycrystals doped with Cr^{2+} and Fe^{2+} ions in the process of solid-phase diffusion. In particular, in an experiment with various laser sources, the Verdet constant was measured for $\text{ZnSe}:\text{Cr}^{2+}$ and $\text{ZnSe}:\text{Fe}^{2+}$ crystals at wavelengths of 632.8, 1064, 1940 and 2430 nm.

2 Characterization of samples

All samples of magneto-active materials used in the experiments were produced from the same initial CVD-ZnSe plate with an average grain size of 70 μm . Four rectangular parallelepiped blanks were cut from the ZnSe-plate: two blanks were prepared for subsequent doping with chromium and iron, one blank was subjected to only mechanical processing (grinding and polishing), and another blank was subjected to additional high isostatic pressure treatment (HIP). Alloying of the samples was carried out from vacuum-deposited metal films of chromium and iron by diffusion annealing in a quartz ampule followed by HIP treatment [18]. It should be noted that despite the prolonged HIP treatment (about 38 h), the $\text{ZnSe}:\text{Fe}^{2+}$ sample had a pronounced non-uniform distribution of the dopant throughout the thickness.

As a result, the following were produced: two samples of pure ZnSe with different average grain sizes (70 and 300 μm), the $\text{ZnSe}:\text{Cr}^{2+}$ and $\text{ZnSe}:\text{Fe}^{2+}$ samples with

non-uniform doping profiles. All samples were made in the form of $5 \times 5 \times 10 \text{ mm}^3$ rectangular parallelepipeds with two polished small edges. In order to measure the transmission spectra and doping profiles of the samples, 2 mm plates were cut from the origin blanks along the doping direction. Transmission spectra in visible and infrared wavelengths obtained using a SF-56 (Lomo) spectrophotometer and a 660-IR (Varian) Fourier spectrometer are shown in Fig. 1.

It can be seen from Fig. 1, that the transmittance is lower for the doped samples. Transmission losses in the doped samples at the near-wavelength range are associated with strong internal scattering losses, but in the long-wavelength region, losses are not connected with internal non-resonant absorption or scattering, but the polishing quality of the sample surfaces. The works [16, 19] show that doped samples can be manufactured with low optical losses in the entire mid-IR wavelength range. Figure 1. also shows that the transmission spectra of the studied doped samples do not contain absorption lines associated with Cr^{3+} and Fe^{3+} ions.

The studied materials were fabricated in the laboratory of High Purity Laser Materials of ICHPS. The detailed information on X-ray diffraction data and on the content of unwanted impurity for $\text{ZnSe}:\text{Cr}^{2+}$ and $\text{ZnSe}:\text{Fe}^{2+}$ polycrystals, created in ICHPS, can be found in related publications, for example [20].

Figure 2 shows the concentration profiles of active ions in the $\text{ZnSe}:\text{Cr}^{2+}$ and $\text{ZnSe}:\text{Fe}^{2+}$ samples, measured according to the method presented in [16], and also points the area through which the probe laser beam passed in our experiment.

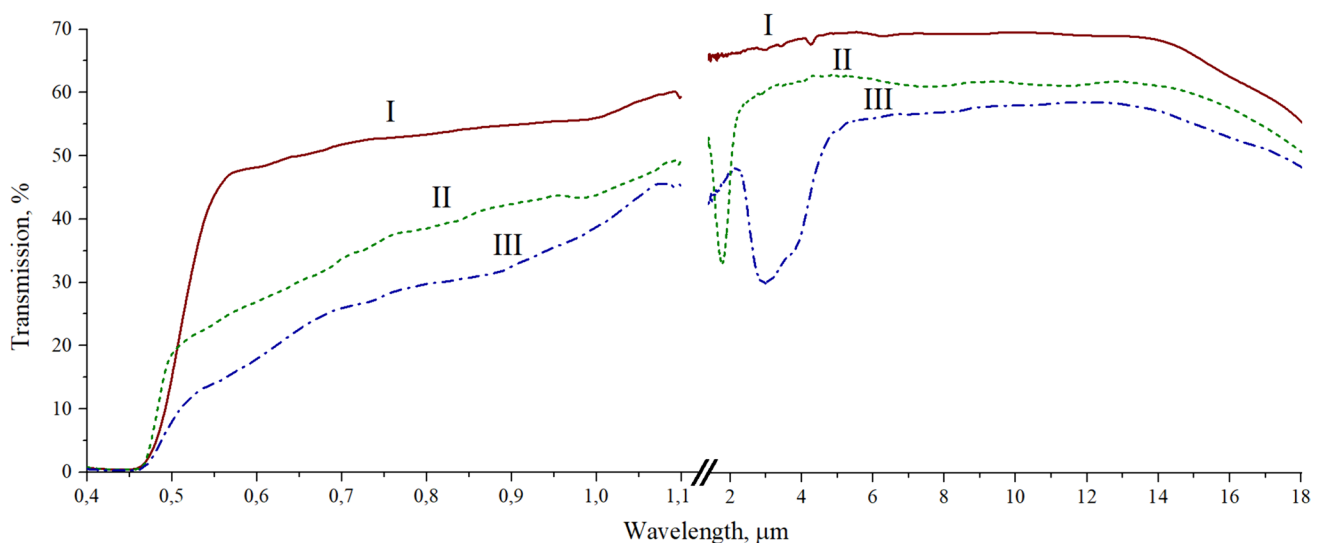


Fig. 1 Vis- and IR-transmission spectra of the samples: I – pure ZnSe; II – $\text{ZnSe}:\text{Cr}^{2+}$; III – $\text{ZnSe}:\text{Fe}^{2+}$. Sample thickness is about 2 mm

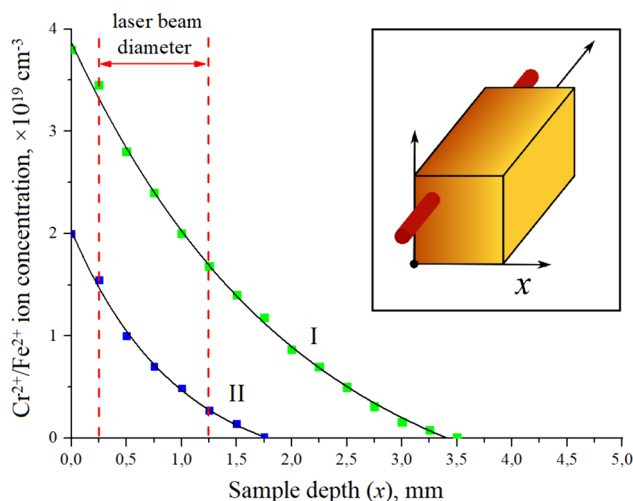


Fig. 2 Distribution of the active ions into the ZnSe:Cr²⁺ (I) and ZnSe:Fe²⁺ (II) samples, and the sample position relative to the probe beam in the experiment (inset)

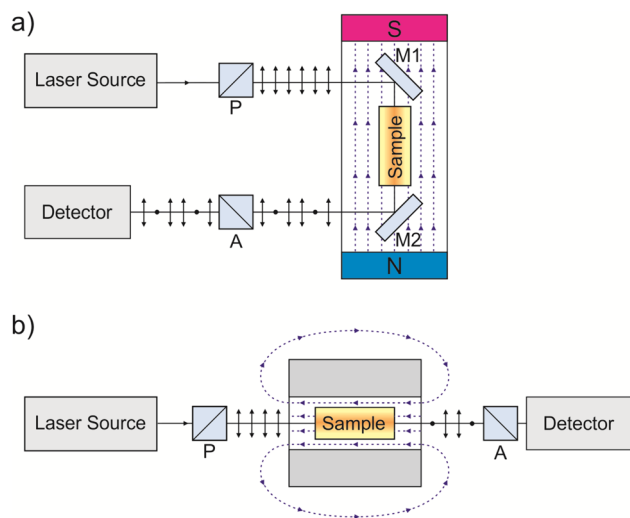


Fig. 3 Experimental setup: (a) – with a probe beam at wavelengths of 632 and 1064 nm; (b) – with a probe beam at wavelengths of 1940–2430 nm

3 Experiment

The measurement of Faraday rotation in samples involved the use of laser sources operating in both the visible and IR wavelength ranges, so the experiment was carried out in two stages.

In the first stage, to determine the Verdet constant at wavelengths of 632.8–1064 nm, HRR005 He–Ne (Thorlabs) and home-made Nd:YAG lasers were used. In the experiment (Fig. 3a), the probe beam was linearly polarized by the input Glan-Taylor prism (P) and then passed

through the test sample, which was placed between two flat mirrors (M1, M2). The mirrors and magneto-active crystal were placed inside an external constant magnetic field of 0.27 T, which caused a rotation of the polarization of the propagating probe beam. The probe beam radius on the sample was about 500 μm for both laser sources. The average power of probe beam was about 3 mW and 50 mW, when using the He–Ne laser and Nd:YAG laser, respectively.

The detection system consisted of a Glan-Taylor prism (A), which could be rotated around the optical axis and was used as an analyzer, and a PDA36A/M photodetector (Thorlabs) (in the case of the He–Ne laser) or a S302C laser power meter (Thorlabs) (in the case of the Nd:YAG laser). First, for calibration, a probe beam was passed through the sample in the absence of a magnetic field. Then the analyzer was rotated so that the probing laser radiation did not pass through it. Next, the sample was placed in the permanent magnetic field, and a new angular position was found at which the analyzer did not transmit radiation. The difference between these two angular positions of the analyzer determined the polarization rotation angle θ . From this the Verdet constant at room temperature was calculated by:

$$\theta = VBL \tag{1}$$

where L – sample length, B – magnetic field value.

At the next stage, Verdet constants were determined for the same samples at wavelengths of 1940–2430 nm. For this purpose, the CW home-made Tm:YAP and Cr:ZnSe lasers were used as radiation sources. In the case of the Cr:ZnSe laser, the spectral width of the radiation at half maximum was about 20 nm with a maximum at 2430 nm, while the Tm:YAP laser had a narrow band spectrum with FWHM of 1 nm. The experimental setup was simplified and the magnetic field was enhanced by using a hollow cylinder-shaped magnet with on-axis magnetic field of 0.8 Tesla (Fig. 3b). The sample was placed between two Glan-Taylor prisms: a polarizer (P), which controlled the probe beam polarization, and an analyzer (A), which was rotated to determine the change in polarization. The Verdet constant was also calculated using formula (1).

The results of the calculations are summarized in Table 1. The values are given taking into account the total error, which included instrumental and random measurement errors. It turned out that instrument error had the greatest impact on the measurement accuracy in our experiments. In addition, for doped samples, it is necessary to take into account a significant concentration gradient in the direction perpendicular to the probing beam (Fig. 2). The table shows the average concentration values N for the ZnSe:Cr²⁺ and ZnSe:Fe²⁺ samples.

Table 1 Measured values of Verdet constants for the studied samples

Sample	V [rad/T•m] @ 632.8 nm	V [rad/T•m] @ 1064 nm	V [rad/T•m] @ 1940 nm	V [rad/T•m] @ 2430 nm
ZnSe (grain size 70 μm)	98 ± 8.9	27.3 ± 2.7	9 ± 0.4	4.3 ± 0.4
ZnSe (grain size 300 μm)	96 ± 8.7	27.1 ± 2.7	9.1 ± 0.4	4.2 ± 0.4
ZnSe (data from [15])	98.5	28.3	7.7	–
ZnSe:Cr ²⁺ ($N=2.5 \times 10^{19} \text{ cm}^{-3}$)	137 ± 12.5	30.5 ± 3.0	–	5.3 ± 0.4
ZnSe:Fe ²⁺ ($N=0.8 \times 10^{19} \text{ cm}^{-3}$)	139 ± 12.6	35 ± 3.4	11.5 ± 0.5	6.2 ± 0.4

4 Discussion

The results of our work for pure ZnSe polycrystals are in good agreement with the results of work [15] for single crystals (Table 1). As can be seen from Table 1, for the pure ZnSe samples, the difference in grain size did not affect their magneto-optical properties, and both samples demonstrated similar results. Pure ZnSe has a Verdet constant of 98 rad/(T•m) at 632.8 nm, that is lower than the values for CeF₃ (~ 123 rad/(T•m)), TGG (~ 130.6 rad/(T•m)) and Dy₂O₃ (~ 247.6 rad/(T•m)) [4]. At 1064 nm, the Verdet constant of ZnSe is about 27 rad/(T•m), that is also less than 39 rad/(T•m) for CeF₃ and some other rare earth materials. However, the values of the Verdet constant at 1940 nm for ZnSe and CeF₃ are almost the same [7].

In general, the dispersion of the Verdet constant of ZnSe (pure or doped with transition metals) in a wavelength range below the fundamental absorption edge can be described as:

$$V = \frac{A}{\lambda^2 - \lambda_0^2} \quad (2)$$

where A and λ_0 – fitting factors determined by a specific magneto-active material [15]. This dependence can be useful in calculations of Faraday devices in the long-wave spectral range.

According to studies [21, 22], the Verdet constant of doped materials can be expressed as

$$V(\lambda) = xV_{para}(\lambda) + (1 - x)V_{dia}(\lambda), \quad (3)$$

where $V_{dia}(\lambda)$ refers to the contribution of the diamagnetic, and $V_{para}(\lambda)$ – the contribution of the paramagnetic and x is the content of dopant.

So the enhanced Faraday rotation in diffusion doped ZnSe:Cr²⁺ and ZnSe:Fe²⁺ can be explained by the Van Vleck-Hebb theory for paramagnets [22–24]. According to this theory, the paramagnetic component of the Verdet constant can be defined as:

$$V_{para} = \frac{4\pi^2\nu^2\chi}{g_s\mu_Bch} \sum_{ij} \frac{C_{ij}}{\nu^2 - \nu_{ij}^2} \quad (4)$$

where ν is the incident light frequency, χ is the magnetic susceptibility, g_s is the Landé factor, μ_B is the Bohr magneton, c is the speed of light in vacuum, h is the Planck constant; C_{ij} related to the transition probability and ν_{ij} is the frequency of electronic transitions. Numerical calculation using the formula (4) is complicated due to the large number of transitions between electronic states. However, for magnetic susceptibility, under some approximations, the following expression is valid [25]:

$$\chi = \frac{N\mu_0g_s^2S(S+1)\mu_B^2}{3K_B(T - T_c)} \quad (5)$$

where N is the concentration of dopants, μ_0 is the vacuum permeability, S is the angular momentum quantum number, K_B is the Boltzmann constant, T is the absolute temperature, and T_c is the paramagnetic Curie temperature. According to the formulas (4–5), a Verdet constant linearly depends on the concentration of transition metals dopants. This dependence was observed in our experiment (for the ZnSe:Fe²⁺ polycrystal), when we passed a probe beam through areas of the sample with a lower doping level and obtained a lower (compared to that presented in Table 1) value of the Verdet constant. It should be noted that doping the CdMnTe crystal with iron at a level of $5 \times 10^{19} \text{ cm}^{-3}$ had a pronounced positive effect on the magneto-optical properties [26], which strengthens the confidence that Fe²⁺ is a promising dopant for magneto-optical applications.

5 Conclusions

As a result of the work, it was shown that diffusion doping of ZnSe with Cr²⁺ and Fe²⁺ ions increases the value of the Verdet constant, especially in the long-wavelength spectral

range. The most significant change was achieved on a highly doped ZnSe:Fe²⁺ sample – the relative increase in the Verde constant value at a wavelength of 2430 nm was about 45%. The results obtained indicate the prospects of using zinc chalcogenides as magneto-optical materials for Faraday devices in the mid-IR range.

Acknowledgements The experiments with the Nd:YAG and He-Ne lasers were carried out with the support of the Ministry of Science and Higher Education of the Russian Federation (Project No. 075-15-2022-293). The measurements with the Tm:YAP laser and the Cr:ZnSe laser were performed with the support of Russian Science Foundation (Project No. 20-12-00114).

Author contributions R.Shahin, O. V. Martynova conducted experiments. A. P. Savikin and S. V. Kurashkin wrote the main manuscript and O. V. Martynova prepared figures. All authors reviewed the manuscript.

Funding The experiments with the Nd:YAG and He-Ne lasers were carried out with the support of the Ministry of Science and Higher Education of the Russian Federation (Project No. 075-15-2022-293). The measurements with the Tm:YAP laser and the Cr:ZnSe laser were performed with the support of Russian Science Foundation (Project No. 20-12-00114). The authors have no relevant financial or non-financial interests to disclose.

Data availability The datasets generated during and/or analyzed during the current study are available from the corresponding author on reasonable request.

Declarations

Competing interests The authors declare no competing interests.

References

1. A.K. Zvezdin, V.A. Kotov, *Modern Magneto-optics and Magneto-optical Materials* (Taylor & Francis Group, New York, 1997)
2. R. Yasuhara, H. Nozawa, T. Yanagitani, S. Motokoshi, J. Kawana, *Opt. Express* **21**, 31443 (2013)
3. H. Yoshida, K. Tsubakimoto, Y. Fujimoto, K. Mikami, H. Fujita, N. Miyanaga, H. Nozawa, H. Yagi, T. Yanagitani, Y. Nagata, H. Kinoshita, *Opt. Express* **19**, 15181 (2011)
4. D. Vojna, O. Slezák, A. Lucianetti, T. Mocek, *Appl. Sci.* **9**, 3160 (2019)
5. D. Vojna, R. Yasuhara, O. Slezák, J. Mužík, A. Lucianetti, T. Mocek, *Opt. Eng.* **56**, 067105 (2017)
6. T. Hayakawa, M. Nogami, N. Nishi, N. Sawanobori, *Chem. Mater.* **14**, 3223 (2002)
7. V. Vasylyev, E.G. Villora, M. Nakamura, Y. Sugahara, K. Shimamura, *Opt. Express* **20**, 14460 (2012)
8. P. Molina, V. Vasylyev, E.G. Villora, K. Shimamura, *Opt. Express* **19**, 11786 (2011)
9. D. Vojna, O. Slezák, R. Yasuhara, H. Furuse, A. Lucianetti, T. Mocek, *Materials* **13**, 5324 (2020)
10. T. Sekijima, H. Kishimoto, T. Fujii, K. Wakino, M. Okada, *Jpn. J. Appl. Phys.* **38**, 5874 (1999)
11. M. Mollaei, X. Zhu, S. Jenkins, J. Zong, E. Temyanko, R. Norwood, A. Chavez-Pirson, M. Li, D. Zelmon, N. Peyghambarian, *Opt. Express* **28**, 11789 (2020)
12. M. Mollaei, P. Lucas, J. Ari, X. Zhu, M. Lukowski, T. Manzur, N. Peyghambarian, *Opt. Lett.* **45**, 2183 (2020)
13. I. Snetkov, A. Yakovlev, *Opt. Lett.* **47**, 1895 (2022)
14. S.S. Balabanov, E.M. Gavrishchuk, V.B. Ikonnikov, S.A. Rodin, D.V. 2014 Savin: Method for producing doped zinc chalcogenides (Patent application PCT/RU2014/000605)
15. E.A. Mironov, O.V. Palashov, I.L. Snetkov, S.S. Balabanov, *Laser Phys. Lett.* **17**, 125801 (2020)
16. S.V. Kurashkin, O.V. Martynova, D.V. Savin, E.M. Gavrishchuk, S.S. Balabanov, V.V. Sharkov, *Laser Phys. Lett.* **16**, 075801 (2019)
17. D.V. Savin, T.S. Tomilova, S.V. Kurashkin, V.B. Ikonnikov, E.M. Gavrishchuk, *Laser Phys. Lett.* **17**, 125802 (2020)
18. E. Gavrishchuk, V. Ikonnikov, T. Kotereva, D. Savin, S. Rodin, E. Mozhevitina, R. Avetisov, M. Zykova, I. Avetissov, K. Firsov, S. Kazantsev, I. Kononov, P. Yunin, *J. Crystal Growth* **468**, 655 (2017)
19. N.A. Timofeeva, E.M. Gavrishchuk, D.V. Savin, S.A. Rodin, S.V. Kurashkin, V.B. Ikonnikov, T.S. Tomilova, *Inorg. Mater.* **55**, 1201 (2019)
20. E. Gavrishchuk, M. Zykova, E. Mozhevitina, R. Avetisov, V. Ikonnikov, D. Savin, S. Rodin, K. Firsov, S. Kazantsev, I. Kononov, I. Avetissov, *Phys. Status Solidi* (2017). <https://doi.org/10.1002/pssa.201700457>
21. V. Letellier, A. seignac, A. Le floch, *J. Non-Crystalline Solids* (1989). [https://doi.org/10.1016/0022-3093\(89\)90423-7](https://doi.org/10.1016/0022-3093(89)90423-7)
22. J.H. van Vleck, *The theory of Electric and Magnetic Susceptibilities* (Oxford Univ. Press, Great Britain, 1932)
23. J. Vleck, M. Hebb, *Phys. Rev.* **46**, 17 (1934)
24. A.J. Helbers, *Magneto-Optical Properties of Rare-Earth Doped semiconductors* (Bethlehem, Pennsylvania, Lehigh University, United States, 2017)
25. C. Kittel, *Introduction to Solid State Physics*, 8th edn. (John Wiley & Sons Inc, New York, 2005)
26. W. Palosz, S. Trivedi, H. Prasad, H. Garcia, *J. Electron. Mater.* **52**, 1385 (2023)

Publisher's Note Springer Nature remains neutral with regard to jurisdictional claims in published maps and institutional affiliations.

Springer Nature or its licensor (e.g. a society or other partner) holds exclusive rights to this article under a publishing agreement with the author(s) or other rightsholder(s); author self-archiving of the accepted manuscript version of this article is solely governed by the terms of such publishing agreement and applicable law.